

# Binding of therapeutic Fc-fused factor VIII to the neonatal Fc receptor at neutral pH associates with poor half-life extension

Alejandra Reyes-Ruiz,<sup>1</sup> Sandrine Delignat,<sup>1</sup> Aishwarya Sudam Bhale,<sup>2</sup> Victoria Daventure,<sup>1</sup> Robin V. Lacombe,<sup>1</sup> Leslie Dourthe,<sup>1</sup> Olivier Christophe,<sup>3</sup> Sune Justesen,<sup>4</sup> Krishnan Venkataraman,<sup>2</sup> Jordan D. Dimitrov<sup>1</sup> and Sebastien Lacroix-Desmazes<sup>1</sup>

<sup>1</sup>Institut National de la Santé et de la Recherche Médicale, Centre de Recherche des Cordeliers, CNRS, Sorbonne Université, Université Paris Cité, Paris, France; <sup>2</sup>Center for Bio-Separation Technology (CBST), Vellore Institute of Technology (VIT), Vellore, Tamil Nadu, India; <sup>3</sup>Laboratory for Hemostasis, Inflammation and Thrombosis, Unité Mixte de Recherche 1176, Institut National de la Santé et de la Recherche Médicale, Université Paris-Saclay, Le Kremlin-Bicêtre, France and <sup>4</sup>Immunitrack Aps, Copenhagen, Denmark

**Correspondence:** S. Lacroix-Desmazes  
[sebastien.lacroix-desmazes@inserm.fr](mailto:sebastien.lacroix-desmazes@inserm.fr)

**Received:** August 30, 2024.  
**Accepted:** December 5, 2024.  
**Early view:** December 12, 2024.

<https://doi.org/10.3324/haematol.2024.286536>

©2025 Ferrata Storti Foundation

Published under a CC BY-NC license



## **Supporting Information**

### **Supplemental Methods**

**Sources of antibodies.** Genes encoding the VL and VH regions of human anti-HIV m66.6 IgG was given by Hugo Mouquet (Institut Pasteur, France) and cloned in eukaryotic expressing vectors. The human anti-HIV VRC01-class DRVIA7 IgG expressing plasmids were obtained through the NIH AIDS Reagent Program (Division of AIDS, NIAID, at the National Institutes of Health). Antibodies were expressed in ExpiCHO cells transiently transfected with the different constructs (Thermo Scientific). After 8 days of culture in serum free conditions, supernatants were collected, and antibodies were purified by affinity chromatography (HiTrap MabSelect PrismA, GE Healthcare) using a Fast Protein Liquid Chromatography system (FPLC, Holmes Analytical). The final products were buffer-exchanged to PBS, pH 7.4 using Slide A-lyser dialysis cassettes (Thermo Scientific). Both mAbs shared an identical Fc.

**FcRn binding by surface plasmon resonance.** The binding of Fc-fused proteins to the human and mouse FcRn were studied by surface plasmon resonance using a Biacore 2000 (Cytiva). Biotinylated hFcRn or mFcRn (kind gift from Dr Sune Justesen, Immunitrack, Danemark) were diluted in tris-citrate buffer (100 mM Tris, 100mM NaCl, 5% glycerol and 0.1% tween 20 at pH 6 or pH 7.4) and immobilized on a streptavidin-coated sensor chip at a protein surface density of about 0.5 ng/mm<sup>2</sup> (450–550 RU). Fc-fused proteins were diluted in running buffer (100 mM Tris, 100 mM NaCl, 5% glycerol and 0.1% tween 20, pH 6 or 7.4) and injected at 25°C. The injections were performed using the KINJECT mode (flow,

30  $\mu$ l/min; volume, 120  $\mu$ l; dissociation time, 300 s). For regeneration, 15  $\mu$ l of 100 mM Tris, 100 mM NaCl pH 7.8 (regeneration buffer) were injected. For calculation of binding constants at pH 6, the binding was evaluated in 2-fold serial dilutions of the samples (25 to 0.097 nM). Kinetic constants were calculated from the sensorgrams using the 1:1 Langmuir or binding with drifting baseline model of BIAevaluation software. The quality of the fitting of the models was judged by the low values of the  $\chi^2$ , not exceeding the 10% of the highest RU. The equilibrium dissociation constants were calculated from the values of association and dissociation rate constants, as  $K_D = K_d/K_a$ . When indicated, rFVIII<sub>FC</sub> was pre-incubated with VWF at 1/50 FVIII/VWF ratio or 1/1 ratio of (F(ab')<sub>2</sub>) fragments of anti-A2 (BOIIB2 - patent US20070065425A1), anti-C1 (KM33<sup>1</sup>) or anti-C2 (BO2C11<sup>2</sup>) monoclonal IgG at 30 min at 4°C.

**FcRn binding by ELISA.** Biotinylated human or murine FcRn (2  $\mu$ g/mL, Immunitrack, Denmark) were immobilized on streptavidin (10  $\mu$ g/mL) precoated ELISA plates (Thermo Scientific) and previously blocked with synthetic block (Thermo Scientific), 0.1% tween 20. To determine binding to FcRn, the molecules to be tested were diluted in 100 mM Tris, 100 mM NaCl, 0.1% tween 20, at pH 6 or 7.4 and added to the plate. To determine the ionic strength dependence of the binding, the molecules were tested at 2 nM or 0.2 nM, for human and murine FcRn, respectively, in 10 mM HEPES pH 7.1 containing 0, 0.06, 0.125, 0.25, 0.5, or 1 M NaCl. Bound molecules were detected with horse-radish peroxidase (HRP)-conjugated goat F(ab')<sub>2</sub> anti-human Ig (2012-05, Southern Biotech, Anaheim, CA) or, when indicated, FVIII was detected using a mouse monoclonal anti-FVIII A2

domain IgG (GMA8015, Green Mountain, Burlington, VT) and a goat anti-mouse IgG conjugated with HRP (1030-05, Southern Biotech, Birmingham, AL). The 3,3',5,5'-tétraméthylbenzidine (TMB) was used as a substrate. Optical densities were measured at 450 nm with a TECAN Infinite 200.

**Evaluation of surface electrostatic potentials.** The 3D structures of human FcRn (4N0F), human BDD FVIII (6MF2), human anti-HIV m66.6 Fab (4NRZ), human anti-HIV VRC01-class DRVIA7 Fab (5CD5) were obtained from the PDB database (<https://www.rcsb.org/>) <sup>3</sup>. Modeling of the FVIII<sup>C1C2</sup> mutant with the four R2090A, K2092A, F2093A, R2215A mutations was performed using the Iterative Threading Assembly Refinement (I-TASSER) web server (<https://zhanglab.dcm.b.med.umich.edu/I-TASSER/>). This web-based tool utilizes homology modeling techniques to generate 3D structures based on known templates. The model then underwent quality assessment using the SAVES platform (<https://saves.mbi.ucla.edu/>), and their Ramachandran plot distributions were evaluated through the PDBsum server (<https://www.ebi.ac.uk/thornton-srv/databases/cgi-in/pdbsum/>) <sup>4</sup>. Subsequently, the mutant model was subjected to energy minimization using the SWISS-PDB Viewer tool (<https://www.expasy.org/spdbv>) to alleviate internal constraints and reduce the overall potential energy of the model <sup>5</sup>. The surface electrostatic potentials of the proteins and of the modeled BDD FVIII<sup>C1C2</sup> mutant were calculated by the Coulomb computational method using SWISS-PDB viewer.

**Docking of FVIII C1C2 domains and FcRn at pH7.4.** The C1C2 domains of FVIII were modeled using the crystal structure of FVIII (2R7E) as a template through the ITASSER Modelling server (<https://zhanggroup.org/I-TASSER/>). The structure underwent refinement using ProteinPrepare (<https://playmolecule.org/proteinPrepare/>), a web application designed for protein manipulation such as titration and protonation at user-specified pH levels <sup>6</sup>. The solvent pH was set to 7.4 to replicate physiological conditions. Utilizing PROPKA3.1, ProteinPrepare predicted protonation states of residues based on the designated pH, ensuring accurate representation. Simultaneously, the software employed PDB2PQR to optimize hydrogen-bonding networks within the protein structures, promoting stability under the specified pH conditions. The refined C1C2 and FcRn protein structures were then downloaded in PDB format for subsequent docking studies. Protein-protein docking was conducted utilizing the HDock webserver (<http://hdock.phys.hust.edu.cn/>) <sup>7</sup>. This computational approach explores the molecular interactions between the proteins, providing insights into complex formation and strength. Visualization of the docking results was generated using Biovia Discovery Studio and Pymol for 3D representations, while 2D visualizations were generated using PDBsum (<https://www.ebi.ac.uk/thornton-srv/databases/pdbsum/>) <sup>5</sup>.

**In vivo half-life of Fc-fused FVIII variants.** Ten- to 15-week-old FVIII exon 16 knock-out (FVIII-KO) mice and VWF-KO mice on the C57BL/6 background were used. Animals were handled in agreement with local ethical authorities (approved

by Charles Darwin ethics committee #28694-2020121017336521). FVIII- or VWF-KO mice were intravenously injected with 1 µg rFVIII<sup>1C2</sup>Fc (Eloctate<sup>®</sup>, Sanofi) or FVIII<sup>C1C2</sup>Fc. Blood was collected in citrated tubes (Sigma Aldrich) at different time points. Plasma was prepared and kept at -80°C until use. FVIII:Ag was measured by ELISA. For this, ELISA plates were coated overnight at 4°C with 5 µg/mL mouse anti-human IgG Fc antibody (LS-C108752, LifeSpan BioSciences, Shirley, MA). Plasma diluted in PBS-5% BSA was added to the plates. Bound FVIII was detected with a biotinylated mouse monoclonal anti-FVIII A2 domain IgG (GMA8015, Green Mountain), streptavidin conjugated to horse-radish peroxidase (HRP, R&D Systems, Minneapolis, MN) and OPD (o-phenylenediamine dihydrochloride) substrate. Optical densities were measured at 492 nm with a TECAN Infinite 200.

**Von Willebrand factor binding ELISA.** Von Willebrand factor (VWF, Wilfactin, LFB, France) at 2 µg/mL was coated on ELISA plates (Thermo Scientific) overnight at 4°C. The rFVIII<sup>1C2</sup>Fc variants were diluted in PBS-1% milk, 0.1% tween 20 and added to the plates. Bound molecules were detected with a biotinylated mouse monoclonal anti-FVIII A2 domain IgG (GMA8015, Green Mountain), streptavidin conjugated to HRP (R&D Systems) and TMB substrate. Optical densities were measured at 450 nm with a TECAN Infinite 200.

## References

1. van den Brink EN, Turenhout EA, Bovenschen N, et al. Multiple VH genes are used to assemble human antibodies directed toward the A3-C1 domains of factor VIII. *Blood* 2001;97(4):966–972.
2. Jacquemin MG, Desqueper BG, Benhida A, et al. Mechanism and kinetics of factor VIII inactivation: study with an IgG4 monoclonal antibody derived from a hemophilia A

- patient with inhibitor. *Blood* 1998;92(2):496–506.
3. Berman HM, Westbrook J, Feng Z, et al. The Protein Data Bank. *Nucleic Acids Res* 2000;28(1):235–242.
  4. Laskowski RA, Jabłońska J, Pravda L, Vařeková RS, Thornton JM. PDBsum: Structural summaries of PDB entries. *Protein Sci* 2018;27(1):129–134.
  5. Bhale AS, Venkataraman K. Delineating the impact of pathogenic mutations on the conformational dynamics of HDL's vital protein ApoA1: a combined computational and molecular dynamic simulation approach. *J Biomol Struct Dyn* 2023;41(24):15661–15681.
  6. Martínez-Rosell G, Giorgino T, De Fabritiis G. PlayMolecule ProteinPrepare: A Web Application for Protein Preparation for Molecular Dynamics Simulations. *J Chem Inf Model* 2017;57(7):1511–1516.
  7. Yan Y, Zhang D, Zhou P, Li B, Huang S-Y. HDock: a web server for protein-protein and protein-DNA/RNA docking based on a hybrid strategy. *Nucleic Acids Res* 2017;45(W1):W365–W373.

## Supplemental Tables

**Table S1. Non-bonded contacts between FVIII C1C2 domains and FcRn**

<b>Residues in the C1C2 domains</b>	<b>Residues in FcRn</b>	<b>Distance (Å)</b>	<b>FVIII domain</b>
2021	55	2.488	C1
2021	169	4.564	C1
2022	53	4.106	C1
2022	55	3.031	C1
2023	55	4.403	C1
2052	172	3.954	C1
2052	176	3.878	C1
2052	177	4.447	C1
2053	175	3.239	C1
2053	176	3.580	C1
2053	177	2.908	C1
2055	179	3.364	C1
2055	258	2.905	C1
2055	259	2.488	C1
2055	260	3.236	C1
2085	172	3.490	C1
2085	173	4.668	C1



2087	176	4.315	C1
2090	179	4.802	C1
2090	180	2.924	C1
2090	181	2.969	C1
2090	182	4.927	C1
2092	183	4.750	C1
2093	183	3.070	C1
2094	16	4.689	C1
2095	19	4.355	C1
2130	12	4.971	C1
2130	13	4.160	C1
2131	178	4.416	C1
2131	231	4.641	C1
2131	12	3.807	C1
2131	13	3.399	C1
2132	178	2.840	C1
2133	176	2.947	C1
2133	177	3.874	C1
2133	178	2.711	C1
2133	231	4.885	C1
2135	173	4.355	C1
2135	176	3.446	C1
2137	50	4.865	C1

2137	53	2.744	C1
2137	54	4.666	C1
2138	53	4.669	C1
2139	53	3.305	C1
2157	19	4.603	C1
2163	177	4.197	C1
2176	169	4.376	C2
2177	168	3.002	C2
2178	168	4.852	C2
2179	168	3.791	C2
2180	102	4.870	C2
2181	164	4.961	C2
2181	167	4.010	C2
2181	168	3.228	C2
2181	171	1.592	C2
2182	164	3.560	C2
2182	165	3.917	C2
2182	168	2.649	C2
2183	98	2.535	C2
2183	99	4.752	C2
2183	102	2.890	C2
2183	103	4.797	C2
2183	164	2.876	C2

2187	101	4.594	C2
2187	102	4.499	C2
2206	102	4.834	C2
2207	100	3.831	C2
2207	101	2.777	C2
2209	102	3.454	C2
2210	171	4.637	C2
2211	171	3.154	C2
2211	175	3.531	C2
2213	4	2.833	C2
2213	100	4.554	C2
2214	4	4.230	C2
2214	100	4.963	C2
2215	100	4.880	C2
2215	101	4.738	C2
2322	168	3.104	C2

**Table S2. Specific activities of Fc-fused FVIII variants.** FVIII activity was measured by functional chromogenic assay and protein concentration was evaluated by absorbance at 280 nm.

	<b>Specific activity (IU/mg)</b>
rFVIII <sub>Fc</sub>	4265
rFVIII <sup>C1C2</sup> <sub>Fc</sub>	1392-2398
rFVIII <sup>N2118Q</sup> <sub>Fc</sub>	1951

**Table S3. Kinetic parameters for the binding of FVIII<sup>N2118Q</sup>Fc and rFVIII<sup>C1C2</sup>Fc to human and mouse FcR at pH 6.** The binding kinetics of the rFVIII<sup>C1C2</sup>Fc variants were calculated by surface plasmon resonance at pH 6 after injection of serial dilutions of Fc-fused molecules (flow, 30  $\mu$ l/min; volume, 120  $\mu$ l; dissociation time, 300 s) in streptavidin-coated chips with immobilized biotinylated human or mouse FcRn at 500 RU. The values are represented as the range of 2 or 3 independent experiments.

Binding to human FcRn				
	$k_a$ (M <sup>-1</sup> .s <sup>-1</sup> )	$k_d$ (s <sup>-1</sup> )	$K_D$ (nM)	Chi <sup>2</sup>
rFVIII <sup>C1C2</sup> Fc	6.5-8.1x10 <sup>5</sup>	2.1-2.4x10 <sup>-3</sup>	2.6-3.6	<13
rFVIII <sup>N2118Q</sup> Fc	1.2-1.6x10 <sup>6</sup>	1.7-3.0x10 <sup>-3</sup>	1.0-2.6	<7.0
Binding to murine FcRn				
	$k_a$ (M <sup>-1</sup> .s <sup>-1</sup> )	$k_d$ (s <sup>-1</sup> )	$K_D$ (nM)	Chi <sup>2</sup>
rFVIII <sup>C1C2</sup> Fc	6.0-6.1x10 <sup>5</sup>	1.2-2.2x10 <sup>-4</sup>	0.2-0.36	<3.5
rFVIII <sup>N2118Q</sup> Fc	1.0-1.2x10 <sup>6</sup>	2.1-2.9x10 <sup>-4</sup>	0.2-0.25	<4.0

## Supplemental Figures

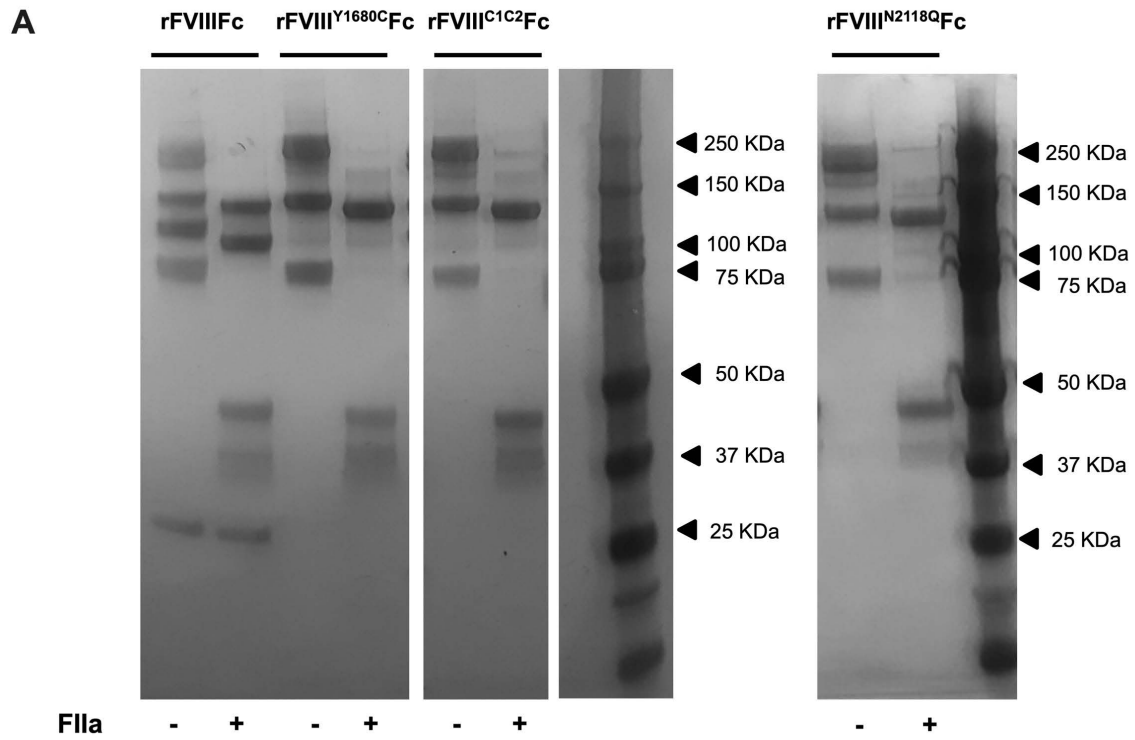


**Figure S1.** SDS-PAGE of rFVIII-Fc, FVIII<sup>Y1680C</sup>-Fc, FVIII<sup>C1C2</sup>-Fc or FVIII<sup>N2118Q</sup>-Fc with and without prior exposure to thrombin (FIIa, 1U).

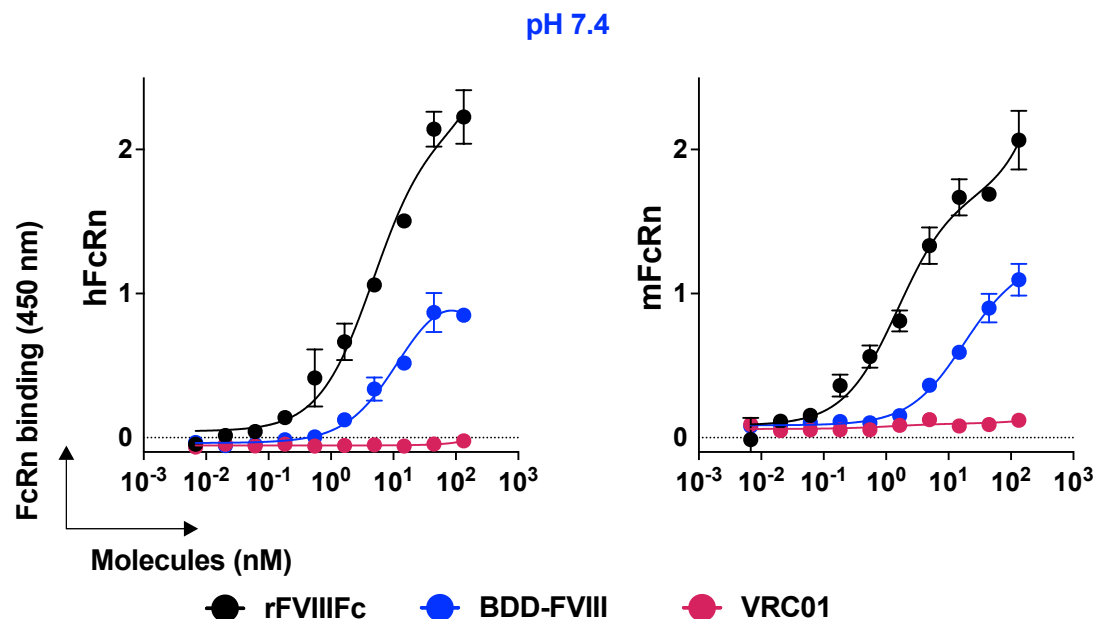


**Figure S2.** Binding of rFVIII Fc or BDD-FVIII (0.007-133 nM) to human (left) or murine (right) FcRn by ELISA at pH 7.4. The molecules were incubated in serial dilutions on plates coated with FcRn. The graphs depict the binding of the FVIII proteins using a mouse monoclonal anti-FVIII A2 domain IgG (GMA8015) and a goat anti-mouse IgG conjugated with HRP (1030-05). Binding is expressed as arbitrary units (AU) as mean  $\pm$ SD based on the optical density measured at 450 nm in 2 independent experiments. VRC01 was used as negative control.

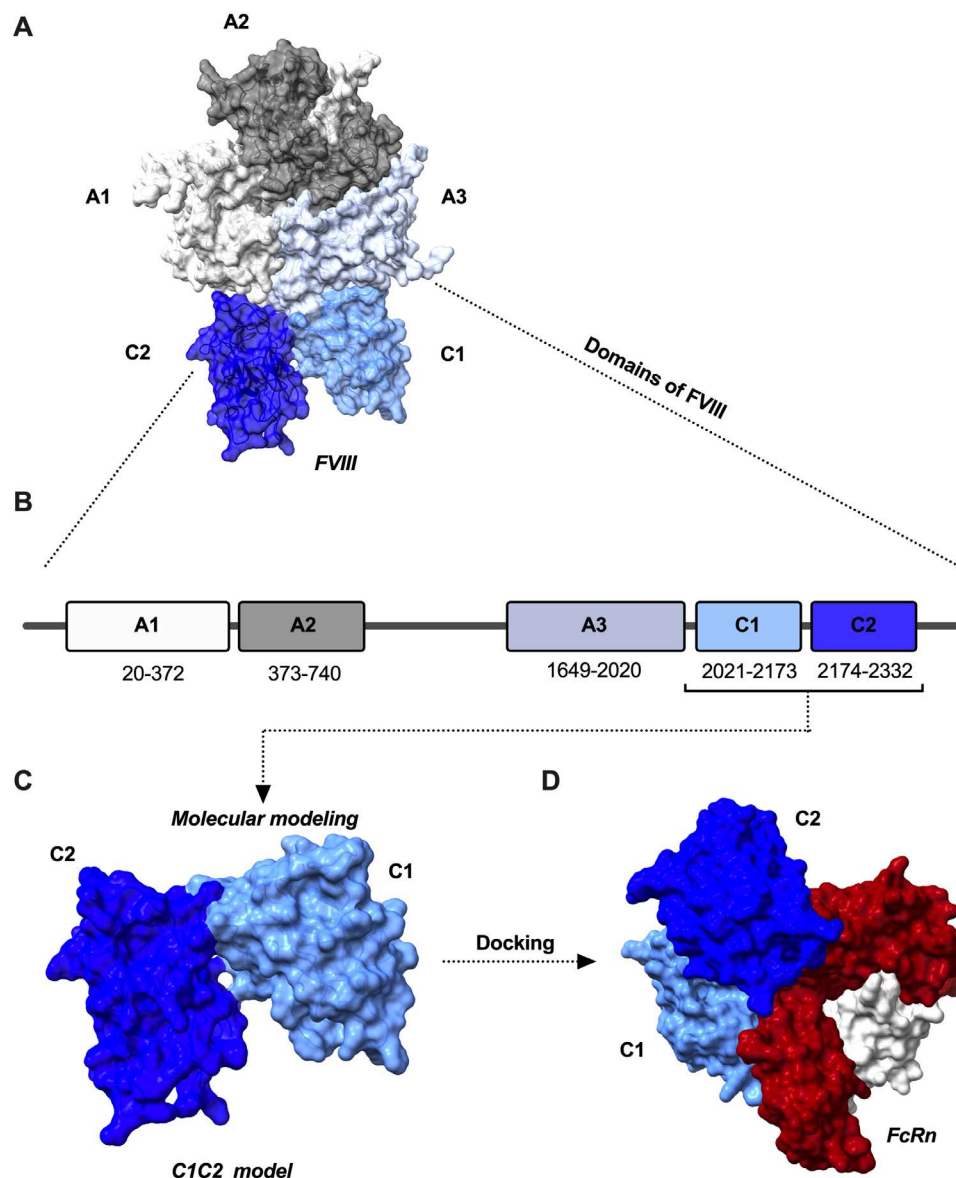


**Figure S3. (A)** Structure of BDD FVIII (PDB: 2R7E), the A1, A2, A3, C1 and C2 domains are depicted in white, gray, light blue, cyan and cobalt blue, respectively. **(B)** BDD FVIII consists of the heavy chain containing the A1 (20-372) A2 (373-740) domains, a truncated B-domain coding the 14-amino acid segment SFSQNPPVLKRHR in place of the B domain (741-1648), and the light chain with A3 (1649-2020), C1 (2021-2173) and C2 (2174-2332) domains. **(C)** Depiction of



C1C2 domains of FVIII modeled using the crystal structure of FVIII (2R7E) as a template through the ITASSER Modelling server. The C1C2 molecular modeling was subjected to quality assessment via the Ramachandran plot using PDBsum server, which predicted 98% of the residues to be in the favored region. (D) Depiction of C1 (cyan) C2 (cobalt blue) domains of FVIII in complex with the light chain  $\beta$ 2 macroglobulin (white) and heavy chain (red) of FcRn (PDB: 4N0F). Protein-protein docking was modeled at pH 7.4 and using the HDOCK webserver.

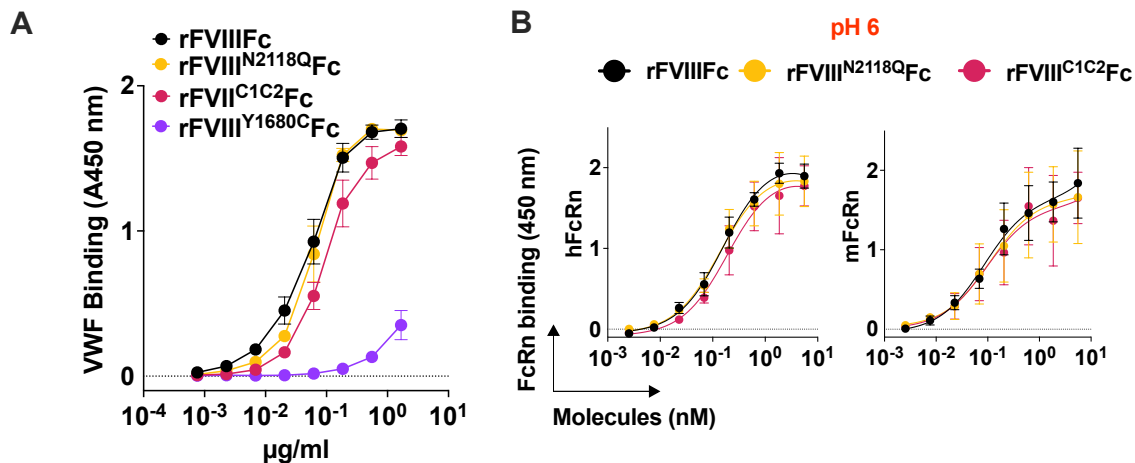


**Figure S4. (A)** Binding of rFVIII Fc variants to VWF by ELISA. The rFVIII Fc variants were incubated in serial dilutions on plates coated with VWF. The graphs depict the binding of the rFVIII Fc variants detected using a biotinylated mouse monoclonal anti-FVIII A2 domain IgG (GMA8015). Binding is expressed as arbitrary units (AU) as mean  $\pm$  SD based on the optical density measured at 450 nm in 2 independent experiments. **(B)** Binding of rFVIII Fc or rFVIII Fc variants (0.0025-5.5 nM) to human (left) or murine (right) FcRn by ELISA at pH 6. The Fc-fused molecules were incubated in serial dilutions on plates coated with FcRn.

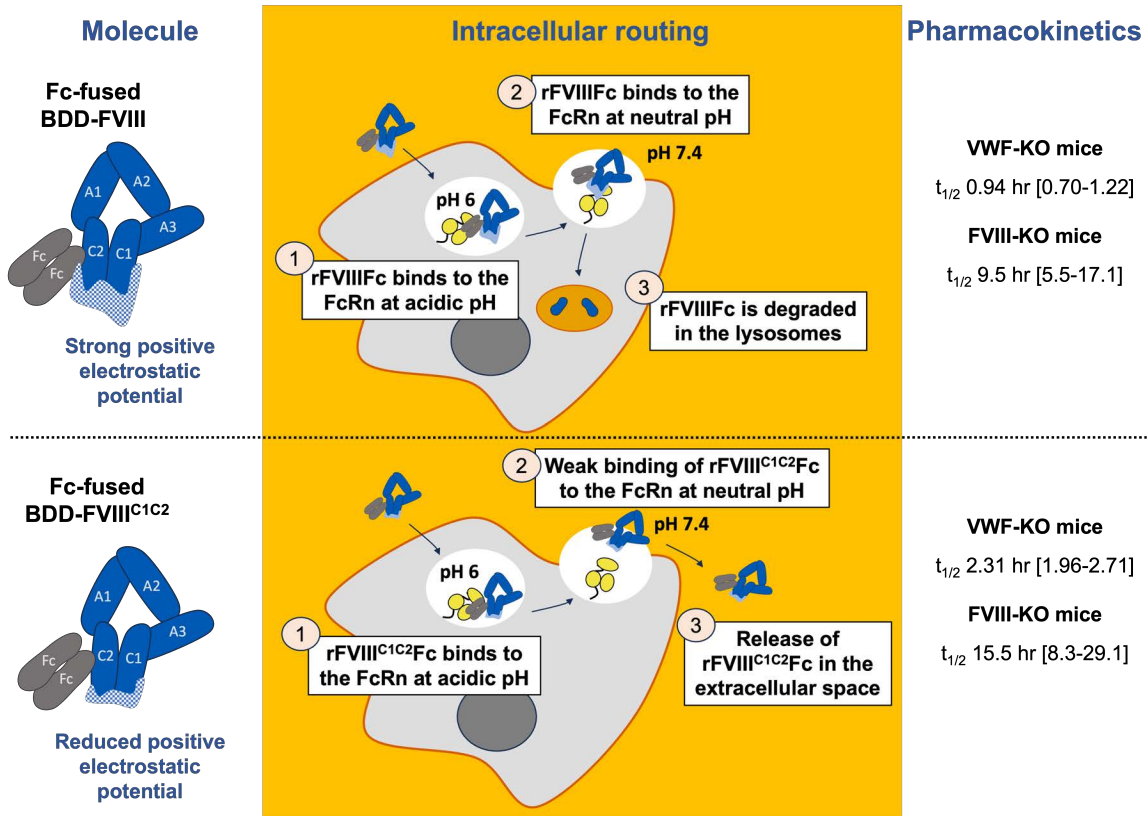


**Figure S5. Visual summary.** Fc-fused BDD-FVIII (rFVIII-Fc) presents a strong positive electrostatic potential, mainly on the surface of the C1 and C2 domains of FVIII (left top panel). The molecule binds to the FcRn at acidic and neutral pH, which prevents the release of the molecule in the extracellular space and could foster its lysosomal degradation (central top panel). Fc-fused BDD-FVIII<sup>C1C2</sup> (rFVIII<sup>C1C2</sup>-Fc) exhibits a reduced positive electrostatic potential (left bottom panel). The molecule binds to the FcRn at acidic pH and presents a weak binding at neutral pH, which allows its release in the extracellular space (central bottom panel). This mechanism participates in the short half-life of rFVIII-Fc (right panel).